Supplementary Figure 1

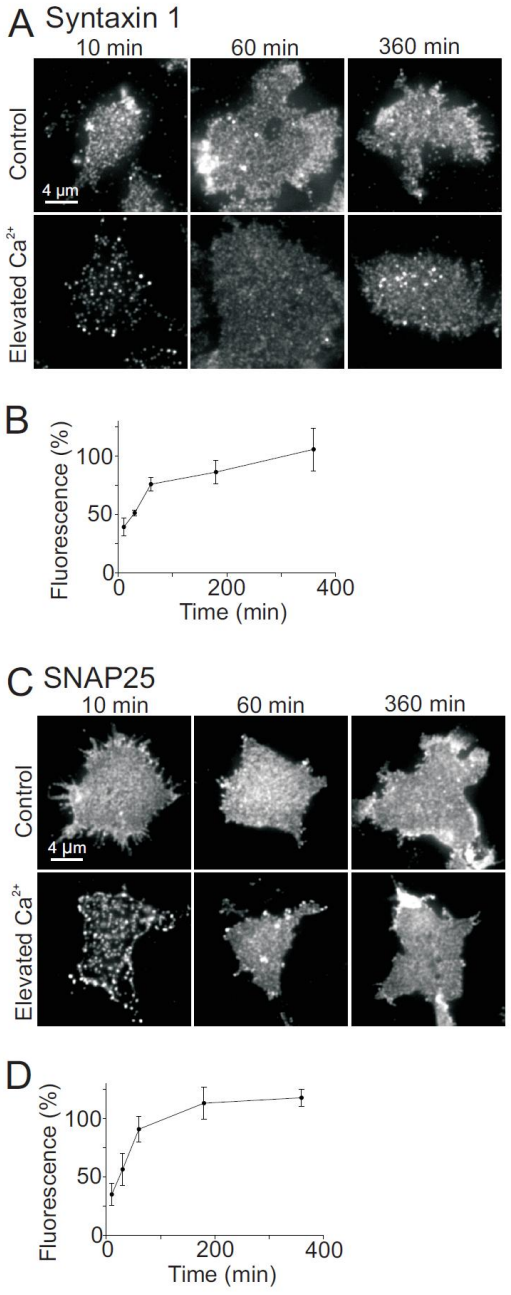

Fig. S1. Recovery of Ca^{2+} diminished syntaxin and SNAP25 immunostaining intensity
PC12 cells were treated for 5 min with 20 µM ionomycin in the presence or absence of extracellular Ca^{2+} and incubated at 37 °C for times as indicated, followed by membrane sheet generation and immunostaining for syntaxin (A + B) or SNAP25 (C + D). Immunofluorescence from stimulated cells was related to the respective control value (set to 100%). Values are given as means ± SEM (n = 3 experiments; 17 - 50 membrane sheets were analyzed for each condition in one experiment).

Supplementary Figure 2

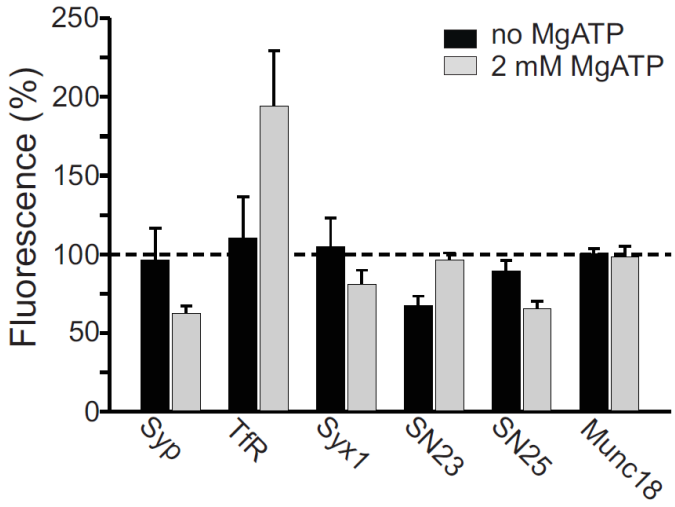

Fig. S2. Influence of the incubation process and Mg^{2+} ions on immunostaining
Freshly prepared membrane sheets were either directly fixed or treated for 5 min without any divalent ions or with 2 mM $MgCl_2$ and 2 mM ATP, fixed and immunostained. For each condition immunofluorescence intensities were normalized to the values obtained from directly fixed membrane sheets. Black bars, incubations in the absence of any ions have no influence on the immunostaining intensity, with the exception of SNAP23 which upon incubation becomes less accessible for immunostaining. Please note that in Fig. 2 the decrease caused by the incubation process (present only in the case of SNAP23) is canceled out by normalization to values from membrane sheets incubated in the absence of Ca^{2+}. Grey bars, addition of magnesium has no clear effect on immunostaining intensities. Values are means ± SEM (n = 3-4 independent experiments; 14-40 membrane sheets were analyzed for each condition in one experiment).

Supplementary Figure 3

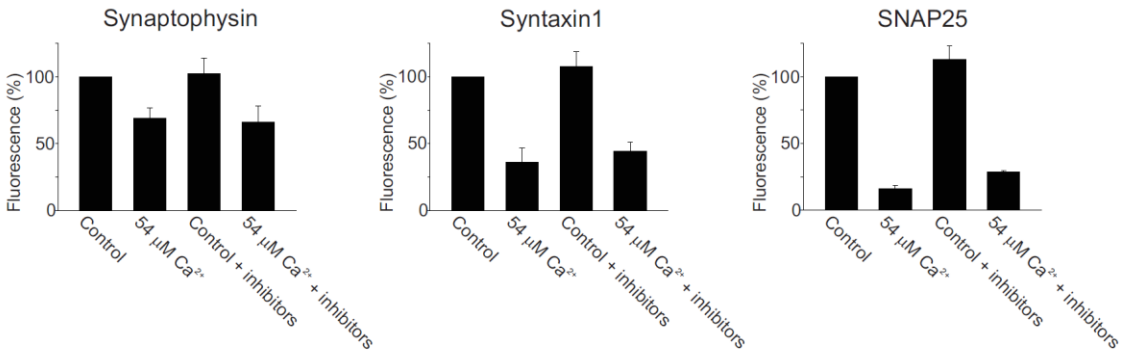

Fig. S3. Ca^{2+} dependent decrease of immunostaining intensity in the presence of protease inhibitors

Membrane sheets were incubated for 10 min with no or 54 µM Ca^{2+} in the absence or presence of a protease inhibitor cocktail (including cocktail complete/Mini/EDTA-free, 1 mM 1,10-Phenanthroline and 1.46 µM Pepstatin A), fixed and immunostained for the proteins as indicated. Data was analyzed as in Fig. 1. Values are given as means ± SEM (n = 3 experiments; 42-74 membrane sheets were analyzed for each condition in one experiment).

Supplementary Figure 4

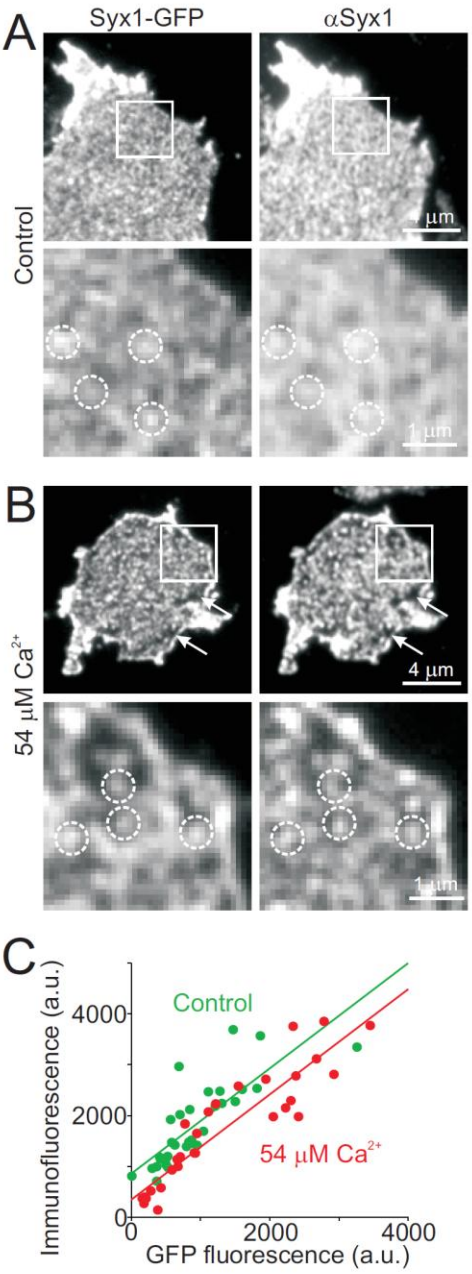

Fig. S4. Syntaxin antibody staining visualizes properly the distribution of syntaxin molecules

(A + B) Membrane sheets from PC12 cells expressing syntaxin 1A-GFP were incubated for 10 min with no (A) or 54 µM (B) Ca^{2+}, fixed and immunostained for syntaxin. For each condition overviews from a membrane sheet in the fluorescent protein (left) and the immunostaining channel (right) are shown. Boxed regions indicate the area from which magnified views are shown. Circles mark identical pixel locations. Closed arrows mark larger areas devoid of syntaxin clusters.

In order to quantify the similarity of the two channels, correlation coefficients between the GFP- and the immunostaining-channels were determined from ROIs placed on the membrane sheets. Analysis yielded values of 0.67 ± 0.01 for the control condition and 0.73 ± 0.01 for 54 μM Ca^{2+}. Values are given as means ± SEM (n = 3 experiments; 10 - 13 membrane sheets were analyzed for each condition in one experiment). Please note that a correlation coefficient of 1 indicates that correlated images are identical. However, in practice instrument noise and imperfect antibody staining produce much lower values though images are supposed to show the same pattern (correlation between myc-staining and GFP-fluorescence from doubly tagged myc-syntaxin 1A-GFP resulted in a correlation coefficient of 0.63 (Sieber et al, 2006)).
(C) From individual control (green dots) and 54 μM Ca^{2+} (red dots) treated membrane sheets GFP-fluorescence was plotted against immunostaining intensity and for each condition a linear regression line was fitted. The data show that under control conditions immunostaining intensity starts from an offset (855 a.u., representing endogenous syntaxin) from which it increases linearly with expression level. Also in the case of 54 μM Ca^{2+} immunostaining intensity increases with expression level but with overall lower intensities (offset value is 342 a.u., or 40 % when compared to control). The magnitude of the Ca^{2+} mediated immunofluorescence decrease is in agreement with experiments in which membrane sheets from non-overexpressing cells were analyzed (compare to Figs. 2B and S3).

Supplementary Figure 5

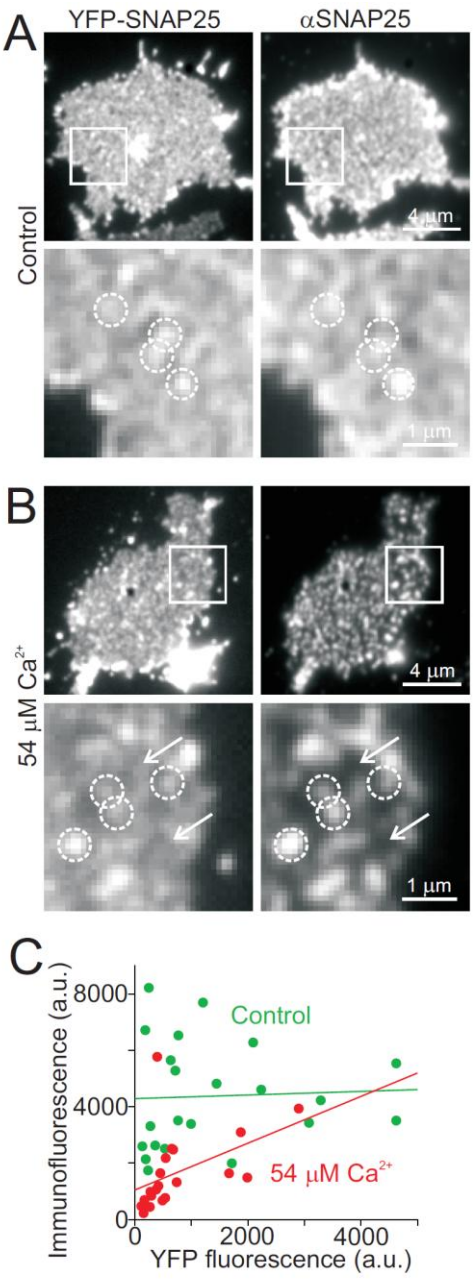

Fig. S5. SNAP25 antibody staining visualizes roughly the clustered SNAP25 distribution and Ca^{2+} masks a more uniformly distributed pool
(A + B) Membrane sheets from PC12 cells expressing YFP-SNAP25 were incubated for 10 min with no or 54 µM (B) Ca^{2+}, fixed and immunostained for SNAP25. Then YFP (left) and immunostaining fluorescence (right) arising from the same membrane sheets were imaged. Shown are overviews (upper panels) and magnified views from the boxed regions of the overviews (lower panels). The open arrows point to areas between SNAP25 clusters where YFP-SNAP25 is present but not efficiently immunostained.

To quantify the similarity of the two channels, correlation coefficients were determined (see also Fig. S4) yielding values of 0.52 ± 0.05 for the control condition and 0.56 ± 0.02 for 54 μM Ca^{2+}. Values are given as means ± SEM (n = 3 experiments; 5 - 10 membrane sheets were analyzed for each condition in one experiment). Please note that the correlation analysis is not sensitive for the disappearance of the masked uniform background.

(C) From individual membrane sheets YFP-fluorescence was plotted against immunostaining fluorescence (green and red dots for control and 54 μM Ca^{2+} membrane sheets, respectively) and for each condition a linear regression line was fitted yielding offsets of 4284 a.u. (control) and 1045 a.u. (54 μM Ca^{2+}). In the case of 54 μM, only at low expression levels immunostaining intensity increases with expression level, leading to an overestimation of the offset value. Taking the latter into account, the data show that at low SNAP25 overexpression levels Ca^{2+} reduces immunofluorescence to a similar degree when compared to experiments in which membrane sheets from non-overexpressing cells were analyzed (compare to Figs. 2B and S3).

The data also show that under control conditions higher expression levels lead essentially to no increase in immunostaining. The observed saturation is probably due to the abundant presence of endogenous SNAP25 at a surface concentration of 7500 SNAP25 molecules per μm^2 (Knowles et al., 2010), allowing for each molecule a staining area of 140 nm^2. Assuming an antibody globular size of 15 nm x 5 nm (San Paulo and Garcia, 2000) and non-uniform SNAP25 distribution, maximal antibody decoration of the membrane sheet could be reached already at endogenous SNAP25 levels. This may explain why a further increase in SNAP25 does not result in stronger immunostaining intensity.

Supplementary Figure 6

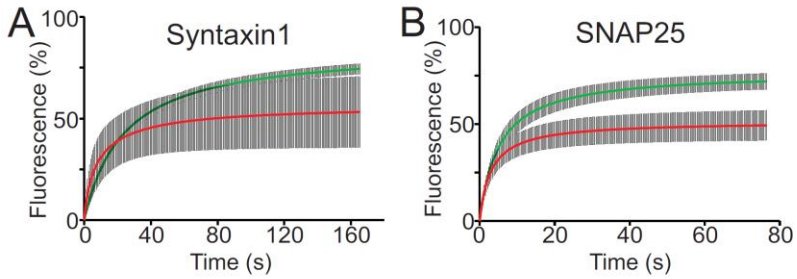

Fig. S6. Determination of maximal recovery and half-times of recovery
For one individual experiment, FRAP recovery curves from 3 - 6 cells were averaged and the average trace was rescaled, setting the pre-bleach value to 100% and the post-bleach value to 0%. The hyperbola function $y(t) = y0 + max_{rec} \times t/(t½ + t)$ was fitted yielding the maximal recovery (max_{rec}) and the half time of recovery (t½). Values obtained for maximal recovery of syntaxin and SNAP25 were 85.1 ± 1.4 % and 76.9 ± 2.1 % before and 56.6 ± 11.7 % and 51.3 ± 4.8 % after elevation of Ca^{2+}, respectively. Values are given as mean ± SEM (n = 3). From the half times of recovery the diffusion coefficients were calculated (shown in Fig. 4E).
For illustration of the overall effect in (A) and (B) only the averages from the fitted graphs are shown. Values are given as mean ± SD (n = 3).

Supplementary Figure 7

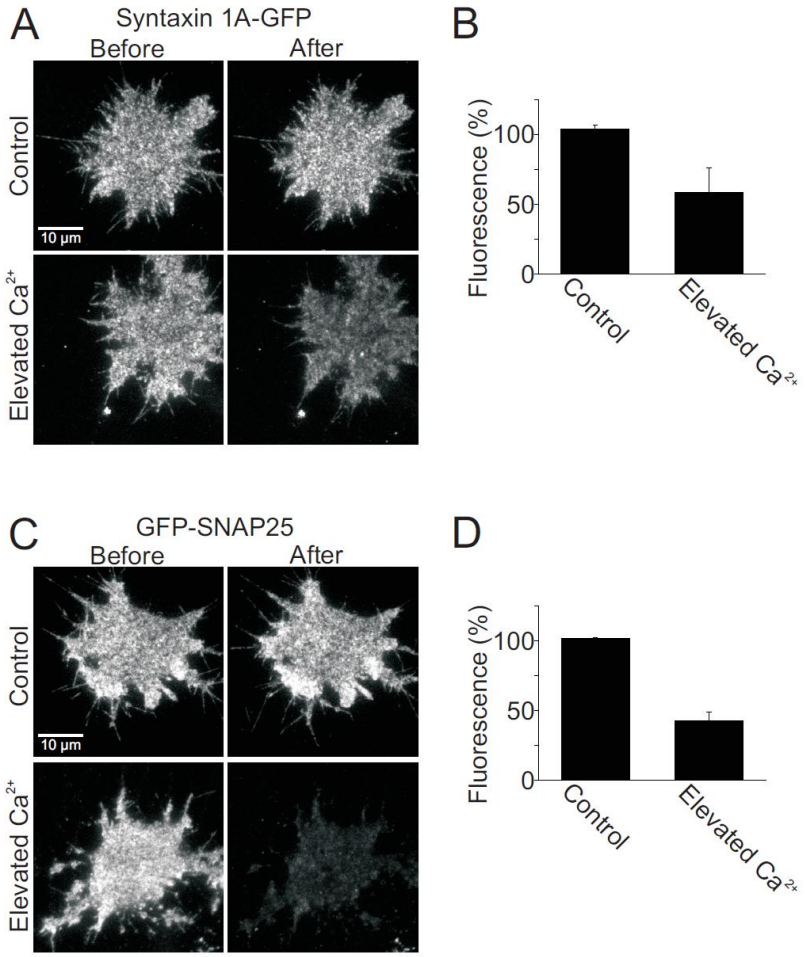

Fig. S7. TIRF-microscopic analysis of the basal plasma membrane after Ca^{2+} treatment
PC12 cells were transfected with syntaxin 1A-GFP (A + B) or GFP-SNAP25 (C + D) and treated with 20 µM ionomycin in the absence (upper panels) or presence (lower panels) of extracellular Ca^{2+}. TIRF micrographs are shown before and 5 min after adding ionomycin. GFP-fluorescence was quantified and values after 5 min were related to the corresponding pre-treatment values. Values are given as means ± SEM (n = 3 experiments; 5 - 7 cells were analyzed for each condition in one experiment).

Supplementary Figure 8

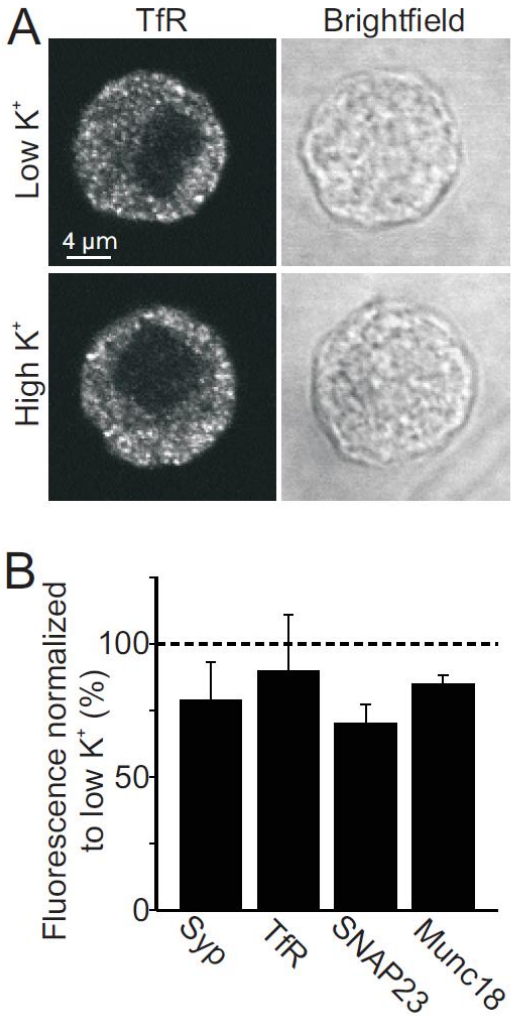

Fig. S8. Effect of depolarization-induced calcium channel opening on immunostaining intensity of synaptophysin, transferrin receptor, SNAP23 and Munc18
Bovine chromaffin cells were treated with low or high potassium Ringer solution for 30 s, fixed, immunostained for the proteins as indicated and analysed by confocal microscopy as described in Fig. 5. Confocal micrographs from equatorial sections in the immunofluorescence (left) and in the brightfield (right) channels are shown for the TfR. Values are means ± SEM (n = 3 independent experiments).

Supplementary Table 1

Table S1. Protein charge distribution analysis

Protein*	Accession No.	Total AA	Cytoplasmic AA **		Cytoplasmic Asp (D), Glu (E)		Cytoplasmic Arg (R), Lys (K)		Δ(%DE-%RK)
			Location	Total	Sum	%	Sum	%	%
Syntaxin1A	P32851	288	1-265	265	57	21.5	45	17.0	4.5
SNAP25B	P60881	206	206	206	43	20.9	29	14.1	6.8
mGFP-SNAP25B	mGFP + RSRAL + P60881	239 + 5 + 206	450	450	34 + 0 + 43	17.1	27 + 2 + 29	12.9	4.2
SNAP23	O70377	210	210	210	35	16.7	26	12.4	4.3
Transferrin Receptor (mouse)	Q62351	763	1-67	67	10	14.9	10	14.9	0.0
Synapto-physin	P07825	307	1-19, 126-132, 219-307	115	10	8.7	8	7.0	1.7
Munc18-1	P61765	594	594	594	85	14.3	81	13.6	0.7

AA: amino acids

* rat sequences were used with the exception of the transferrin receptor for which no full rat sequence was available in the protein database. Instead the mouse sequence was used.

** prediction according to Uniprot.org

Supplementary References

Knowles, M.K., Barg, S., Wan, L., Midorikawa, M., Chen, X. and Almers, W. (2010) Single secretory granules of live cells recruit syntaxin-1 and synaptosomal associated protein 25 (SNAP-25) in large copy numbers. *Proc Natl Acad Sci U S A*, **107**, 20810-20815.

San Paulo, A. and Garcia, R. (2000). High-Resolution imaging of antibodies by tapping-mode atomic force microscopy: attractive and repulsive tip-sample interaction regimes. *Biophys J.* **78**, 1599-1605.

Sieber, J.J., Willig, K.I., Heintzmann, R., Hell, S.W. and Lang, T. (2006) The SNARE motif is essential for the formation of syntaxin clusters in the plasma membrane. *Biophys J*, **90**, 2843-2851.